

ORIGINAL RESEARCH

Open Access



Power generation maximization of distributed photovoltaic systems using dynamic topology reconfiguration

Xiaolun Fang¹, Qiang Yang^{1,2*}  and Wenjun Yan¹

Abstract

The ‘mismatch losses’ problem is commonly encountered in distributed photovoltaic (PV) power generation systems. It can directly reduce power generation. Hence, PV array reconfiguration techniques have become highly popular to minimize the mismatch losses. In this paper, a dynamical array reconfiguration method for Total-Cross-Ties (TCT) and Series-Parallel (SP) interconnected PV arrays is proposed. The method aims to improve the maximum power output generation of a distributed PV array in different mismatch conditions through a set of inverters and a switching matrix that is controlled by a dynamic and scalable reconfiguration optimization algorithm. The structures of the switching matrix for both TCT-based and SP-based PV arrays are designed to enable flexible alteration of the electrical connections between PV strings and inverters. Also, the proposed reconfiguration solution is scalable, because the size of the switching matrix deployed in the proposed solution is only determined by the numbers of the PV strings and the inverters, and is not related to the number of PV modules in a string. The performance of the proposed method is assessed for PV arrays with both TCT and SP interconnections in different mismatch conditions, including different partial shading and random PV module failure. The average optimization time for TCT and SP interconnected PV arrays is 0.02 and 3 s, respectively. The effectiveness of the proposed dynamical reconfiguration is confirmed, with the average maximum power generation improved by 8.56% for the TCT-based PV array and 6.43% for the SP-based PV array compared to a fixed topology scheme.

Keywords: Dynamical reconfiguration, Inverter, Switching matrix, Mismatch losses

1 Introduction

Solar energy is one of the most abundant sources of renewable energy and is becoming an important part of electrical power generation systems worldwide [1, 2]. Statistics [3] indicate that distributed PV systems have grown remarkably faster than large-scale centralized PV farms, and the installed distributed PV capacity in China reached 67.07GW in the first half of 2020. In PV applications, particularly distributed PV systems, the ‘mismatch losses’ problem is one of the main reasons

for power generation degradation. Recent work (e.g., [4]) has found that mismatch losses due to moving clouds are not a major problem of power losses for large-scale PV plants. However, power generation from distributed PV systems will always be affected in urban areas because of the complex environments, e.g. trees, poles, buildings and other objects [1], as illustrated in Fig. 1. Moreover, compared with centralized PV plants, distributed PV systems usually do not have regular inspection and maintenance. Hence some shading caused by dust, bird droppings and fallen leaves and module defects or even failures can persist for a long time. For this reason, two mismatch scenarios, i.e. partial shading scenario and random module failure scenario, are considered for distributed PV systems.

*Correspondence: qyang@zju.edu.cn

¹ College of Electrical Engineering, Zhejiang University, Hangzhou 310027, China

Full list of author information is available at the end of the article



© The Author(s) 2022. **Open Access** This article is licensed under a Creative Commons Attribution 4.0 International License, which permits use, sharing, adaptation, distribution and reproduction in any medium or format, as long as you give appropriate credit to the original author(s) and the source, provide a link to the Creative Commons licence, and indicate if changes were made. The images or other third party material in this article are included in the article's Creative Commons licence, unless indicated otherwise in a credit line to the material. If material is not included in the article's Creative Commons licence and your intended use is not permitted by statutory regulation or exceeds the permitted use, you will need to obtain permission directly from the copyright holder. To view a copy of this licence, visit <http://creativecommons.org/licenses/by/4.0/>.



Fig. 1 Deployment of distributed PV systems with a complex environment

Due to mismatches, PV modules in a PV array may operate at their maximum power points (MPP), resulting in multiple peaks in the output P–V characteristics. This can cause chaos in maximum power point tracking (MPPT) techniques. To address the problem, many studies have adopted PV reconfiguration strategies to reduce mismatch losses. In [5], state-of-the-art reconfiguration strategies for reducing mismatch losses in a PV array are comprehensively reviewed and classified into two categories: static and dynamic reconfiguration techniques. In the static reconfiguration techniques, the physical locations of the PV modules are changed without altering the electrical connection.

In [6] and [7], the physical location of the modules in a 9×9 Total-Cross-Ties (TCT) interconnection of a PV array is rearranged based on the proposed SuDoKu and optimal SuDoKu puzzle patterns. However, the Sudoku puzzle-based reconfiguration technique can only relocate the PV modules within a column, but not change the position in a row. An arrangement of crosses in diagonal view (CDV) is proposed in [8] to distribute the shading effects over the entire PV array for both 9×9 Series–Parallel (SP) and 9×9 TCT interconnections. However, a non-uniform aging phenomenon exists widely in PV generation systems because of the impact of rain, temperature, humidity, and other environmental factors over a long period [9]. As a result, physical relocation is required every few years which demands a lot of labor. Although the static reconfiguration techniques can distribute concentrated shading effects, maximum power generation under all random multiple partial shadows cannot be guaranteed.

In the dynamic reconfiguration techniques, the electrical connections of a PV array can be altered through a set of switches to carry out the reconfiguration. The study in [10] confirms the benefit of these techniques in PV plants through cost–benefit analysis. In general, two options are available to implement the reconfiguration: altering the electrical connections between modules; altering the electrical connections between the modules, the DC/DC converters and the inverters. In the former, a PV array is connected to a

DC/DC converter or an inverter, and the latter allows connecting an adequate number of the strings with a nominated number of DC/DC converters or inverters. Some optimization algorithms, e.g., particle swarm, genetic algorithm (GA), artificial ecosystem-based optimization butterfly ([12–15]), have been adopted to optimize the arrangement of electrical connections of TCT-based PV arrays. In these solutions, each module can be flexibly connected with any other module in the adjacent column by changing the electrical connections with a large number of switches and sophisticated algorithms. To reduce the number of switches, a two-step GA-based PV reconfiguration technique is proposed in [15]. In this method, a PV array is divided into several groups, e.g., a 9×9 PV array can be divided into nine groups of 3×3 . Both the connections between PV modules within the group and the connections among the groups can be altered. However, the number of switches required is dependent on the number of modules in the array. In [16] and [17], the proposed dynamic reconfiguration method uses a switching matrix arranged between fixed and adaptive PV modules that are allowed to be altered in electrical connections with the fixed modules. However, the method cannot improve power generation under certain partial shading patterns, e.g., shading only appears on the fixed modules.

Other solutions are also available to change the electrical connections between the PV modules and DC/DC converters or the inverters to implement the array reconfiguration. A flexible switch matrix is developed in [18] to change the electrical connections between PV modules, a DC/DC converter and a central inverter. In this method, the unshaded PV strings are directly connected to the inverter, and a DC/DC converter is used to connect the remaining modules in the string with partial shading to the inverter. A reconfigured decentralized topology is proposed in [19] for an SP-based PV array. Four DC/DC converters are used and each DC/DC converter is connected to the modules with similar power levels. However, this method also requires deploying a large number of switches, and hence is more suitable for small-scale distributed PV systems.

In summary, the reconfiguration solutions have some obvious limitations. Because of random module defects or failures and the non-uniform aging of the PV modules, the static reconfiguration solutions cannot guarantee maximum power generation under all mismatch conditions. In addition, the dynamic reconfiguration solutions, e.g., [12–16], [18] and [19], always require a large number of switches that significantly increase the installation and maintenance cost as well as the operational complexity. In addition, the dynamic reconfiguration solutions in [16]

and [17] cannot improve power generation under some shadow patterns. The existing dynamic PV array reconfiguration solutions are briefly reviewed and summarized in Table 1.

This paper proposes a dynamic reconfiguration method to address the mismatch losses problem for distributed PV systems. The electrical parameters of individual PV modules can be measured through the deployed voltage and current sensors and made available to the management platform. On the management platform, optimal reconfiguration algorithms are developed to control the switching matrix for dynamic alteration of electrical connections between the PV strings and inverters, rather than the connections between the modules. The main technical contributions of this work can be summarized as follows:

- (1) A dynamical reconfiguration method for TCT-based and SP-based PV arrays is proposed to obtain maximum output power generation of a PV array under mismatch conditions;
- (2) A structural design of switching matrices for both TCT and SP interconnections is presented and the optimal reconfiguration algorithms are developed to control the switching matrix for dynamic alteration of electrical connections between the PV strings and inverters;
- (3) The size of the switching matrix is only determined by the numbers of PV strings and inverters, and is not related to the number of PV modules in a string. Thus, the proposed solution is scalable for a PV array of any size.

Finally, the proposed dynamical reconfiguration algorithmic method is evaluated for a range of partial shading and random PV module failure scenarios.

The remainder of this work is structured as follows: Sect. 2 presents the details of the TCT-based and SP-based PV arrays. Section 3 describes the proposed dynamical reconfiguration method, and the proposed algorithmic solution is assessed and analyzed in Sect. 4. Finally, the conclusion and future work are given in Sect. 5.

2 TCT and SP interconnection PV array

In this work, the mitigation of the mismatch losses problem is investigated through a case study of 9×9 PV arrays with the two most commonly used interconnection schemes: TCT and SP, as illustrated in Figs. 2a, b, respectively. There are 81 PV modules in total in the PV array with 9 rows (strings) and 9 columns, and the label on each PV module indicates its location. For example, the PV module labeled

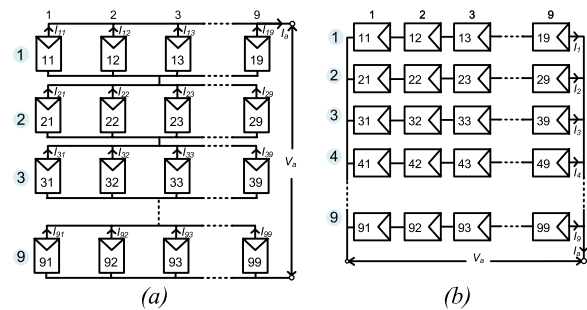


Fig. 2 PV arrays based on 9×9 interconnection scheme: (a) TCT; and (b) SP

Table 1 Summary of dynamic topology reconfiguration solutions

Ref	Reconfiguration solution	Types of mismatch conditions	Configurations	Remarks
[14–17]	Dynamic PV array	Partial shading	TCT	Require a large number of switches: the number of switches depends on the number of modules
[17]	two-step GA-based reconfiguration	Partial shading	TCT	Require a large number of switches: the number of switches depends on the number of modules
[18]	Adaptive bank	Partial shading	TCT	Limit the number of switches: the number of switches depends on the number of PV strings Cannot work well in certain partial shading patterns
[19]	Adaptive bank	Partial shading	SP	Limit the number of switches: the number of switches depends on the number of PV strings Cannot work well in certain partial shading patterns
[20]	Adaptive utility inter-active system	Partial shading	SP	Require a large number of switches: the number of switches depends on the number of modules
[21]	Optimized-String DPVA	Partial shading	SP and TCT	Require a large number of switches: the number of switches depends on the number of modules
This work	Dynamic PV array	partial shading, module failure	SP and TCT	Limit the number of switches: the number of switches depends on the number of PV strings and inverters

‘37’ indicates that the module is located at the 3rd string and the 7th column.

The current limit of the PV module labeled ij is calculated as [20]:

$$I_{ij} = k_{ij}I_m = \frac{G_{ij}}{G_0}I_m \tag{1}$$

where i and j represent the string number and the column number, respectively. I_m is the maximum current produced by a module at the standard irradiance $G_0=1000 \text{ W/m}^2$ and G_{ij} is the irradiance received on the module ij [12].

2.1 TCT-based PV array

As shown in Fig. 2a, in the TCT-based PV array, the modules are connected in parallel in a string and all strings are connected in series [21]. Since the PV modules in a string are connected in parallel, the maximum current produced by each string is equal to the sum of the current limits of all modules. Thus, the maximum current generated by the i th string can be calculated as:

$$I_{stringi,TCT} = \sum_{j=1}^l I_{ij} = \sum_{j=1}^l k_{ij}I_m \tag{2}$$

where l represents the number of PV modules in a string. Since PV strings are connected in series, the current produced by the PV array (I_a) is restricted by the minimum current generation string that is not bypassed ($\min\{I_{stringi,TCT}\}$) [22]. Also, based on Kirchhoff’s voltage law, the voltage of the PV array can be estimated as:

$$V_a = \sum_{i=1}^n V_i \tag{3}$$

where n represents the number of the PV strings and V_i is the voltage of the i th string. The power produced by the PV array can be expressed as:

$$P_a = I_a V_a = \min\{I_{stringi,TCT}\} \times V_a \tag{4}$$

2.2 SP-based PV array

For the SP-based PV array, the PV modules are connected in series in a string and all strings are connected in parallel [23], as illustrated in Fig. 2b. Since PV modules in a string are connected in series, the current produced of the i th string ($I_{stringi,SP}$) is restricted by the minimum current generation module that is not bypassed and the voltage of the i th string (V_i) is the sum of the voltages produced by all modules in a string. Thus, the voltage generation of the i th string can be calculated as:

$$V_i = \sum_{j=1}^l V_{m,ij} \tag{5}$$

where $V_{m,ij}$ is the maximum voltage generation of the PV module labeled ij . Since PV strings are connected in parallel, the voltage generation of the PV array (V_a) is equal to the voltage of each string in parallel and is restricted by the minimum voltage generation string ($\min\{V_i\}$) [24]. Based on Kirchhoff’s circuit law, the current of the PV array (I_a) and the power produced by the PV array can be written respectively as:

$$I_a = \sum_{i=1}^n I_{stringi,SP} \tag{6}$$

$$P_a = I_a V_a = I_a \times \min\{V_i\} \tag{7}$$

3 The proposed dynamical reconfiguration method and algorithms

This section presents in detail the proposed dynamical reconfiguration method to improve the maximum power output of a PV array under mismatch conditions. The algorithmic solutions for two commonly used interconnection schemes, i.e. TCT and SP, are developed and discussed.

3.1 The proposed dynamical reconfiguration method

The proposed method can realize the reconfiguration of PV arrays by altering the electrical connections between strings and inverters without changing the electrical connections of modules and their physical locations. The decision of the dynamic reconfiguration is made based on the real-time electrical parameter measurements of individual PV modules collected by current and voltage sensors, as illustrated in Fig. 3.

Figures 4a and 5a illustrate the TCT-based and SP-based PV arrays combined with a switching matrix and several inverters that can implement the proposed PV array reconfiguration method, respectively. An inverter unit consists of an inverter and one or more PV strings, and each inverter unit is capable of tracking the MPP of its connected PV strings. For both TCT-based and SP-based PV arrays, the size of the switching matrix is only determined by the number of the PV strings and the number of the inverters, and is not related to the number of PV modules in a string. Thus, the proposed solution is scalable for a PV array of any size.

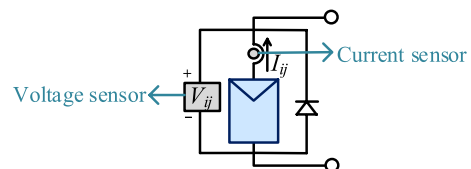


Fig. 3 Position of the electrical parameter measurement sensors in the PV module

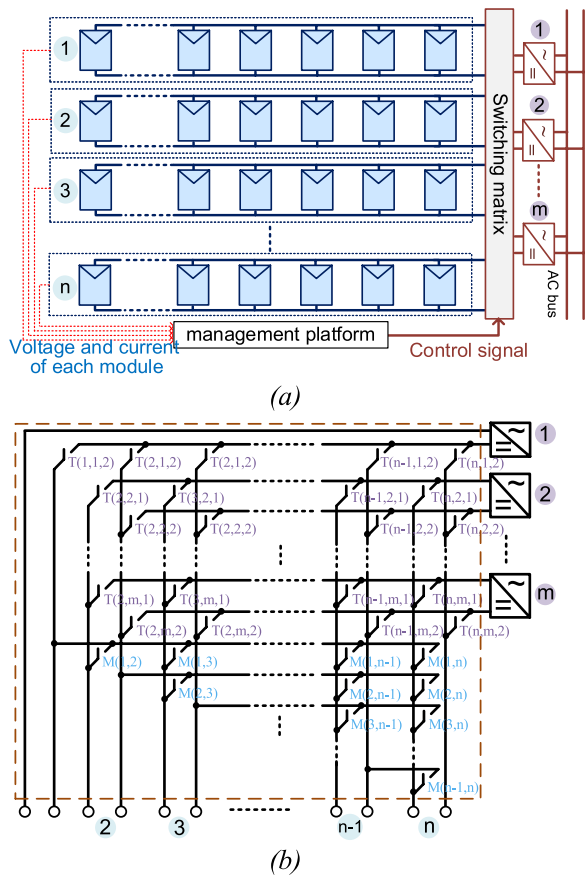


Fig. 4 The proposed method for the TCT-based PV array (a) Interconnection configuration; and (b) designed switching matrix

In the proposed solution, the operation of the switching matrix is determined by the management platform with the dynamic reconfiguration optimization algorithm proposed in Sect. 3.2. That carries out the alteration of electrical connections between PV strings and inverters. The structures of the switching matrices for TCT and SP are shown in Figs. 4b and 5b, respectively. As can be seen, the switching matrix connects n PV strings and n inverters. As shown in Fig. 4b, the switching matrix for TCT contains two switch submatrices $T(i,r,k)$ and $M(i_1,i_2)$, with a total of $2(n-1)(m-1) + n + 0.5n(n-1)$ switches. $T(i,r,k)$ represents the switch that connects the i th PV string to the r th inverter, k represents the interface position of inverters, $k=1$ represents the interface on the upper side and $k=2$ represents the interface on the lower side. $M(i_1,i_2)$ represents the switch that connects the i_1 th PV string to the i_2 th PV string. Additionally, as shown in Fig. 5b, the switching matrix for SP is represented by $S(i,r)$ and contains $m(n-1)$ set of switches. When $S(i,r)$ is in the “closed” state, the i th PV string is connected to the r th inverter in parallel.

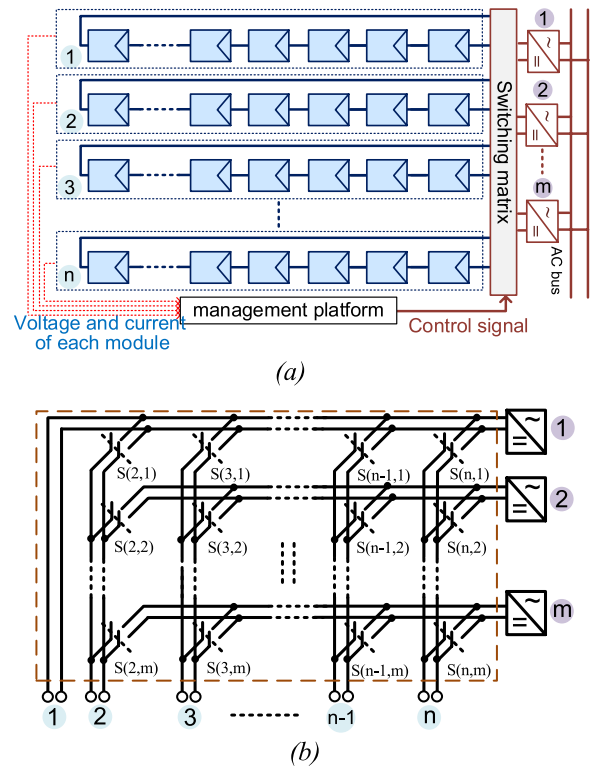


Fig. 5 The proposed method for the SP-based PV array (a) Interconnection configuration; and (b) designed switching matrix

Consequently, for both SP and TCT interconnection schemes, each inverter can be connected to one or more PV strings by controlling the switching matrix. Compared with conventional topology, i.e., where each string has a dedicated inverter (string inverter topology [18]), the number of inverters that need to be deployed in the proposed reconfiguration can be significantly reduced. Also, the PV array using the proposed dynamical reconfiguration can reduce the mismatch losses of the PV array that are due to mismatch phenomena, and hence prevent multiple peaks in the P–V profile of each inverter unit. Thus, the implementation of MPPT can be simplified, and hence the need for sophisticated algorithms can be avoided.

3.2 Application in the TCT-based PV array

In this work, the proposed dynamic reconfiguration algorithmic solution is implemented for an $N \times L$ TCT-based PV array with m inverters, i.e., the PV array consists of a total of n PV strings, m inverters, and l PV modules in each string. The sum of the irradiance at the i th string is represented by G_i which can be calculated as the sum of elements at each string of the matrix \mathbf{G} as:

$$G_i = \sum_{j=1}^l G_{ij} \tag{8}$$

where, G_{ij} can be estimated based on the voltage and current measurements as [25]:

$$G_{ij} = \alpha [I_{ij} + I_0(e^{V_{ij}/\eta V_T} - 1)] \tag{9}$$

In (9), I_{ij} and V_{ij} denote the voltage and current values of the module ij , respectively. α , I_0 and ηV_T are the set of parameters that can be estimated from the manufacturer’s datasheet values [11].

Referring to (1) and (2), the maximum current generated by the i th string can be written as:

$$I_{stringi,TCT} = \sum_{j=1}^l k_{ij} I_m = \frac{G_i}{G_0} I_m \tag{10}$$

Based on (4), the power generated by PV strings connected to the r th inverter can be calculated as:

$$P_{inv,r} = \min\{I_{stringi,TCT,r}\} \times V_{inv,r} \tag{11}$$

where r represents the number of the inverters. $P_{inv,r}$ and $V_{inv,r}$ represent the power output and voltage generation of the r th inverter unit on the DC side, respectively. Here, $\min\{I_{stringi,TCT,r}\}$ represents the minimum string current generation among strings connected to the r th inverter. Then the mismatch losses of the r th inverter unit can be estimated as:

$$P_{loss,r} = \sum_i [I_{stringi,TCT,r} - \min\{I_{stringi,TCT,r}\}] \times V_{inv,r} \tag{12}$$

Based on (12), it can be seen that the current generations of the PV strings connected to an inverter need to be as close as possible to minimize the mismatch losses. Based on (10), in an environment with the same temperature, the string current is proportional to the sum of the irradiance in a string, and hence the algorithm aims to make the total irradiances of individual PV strings as close as possible. In the proposed algorithmic solution, the sum of the irradiance of each string is sorted in ascending order and divided into three groups to connect to three inverters respectively. The idea of searching for the possible connection solutions and two example solutions are illustrated in Fig. 6. In addition, for n PV strings and m inverters, the number of iterations N_{cal} of the algorithm to identify the optimal solution can be expressed as (13):

$$N_{cal} = C_{n-1}^{m-1} = \frac{(n-1)!}{(m-1)!(n-m)!} \tag{13}$$

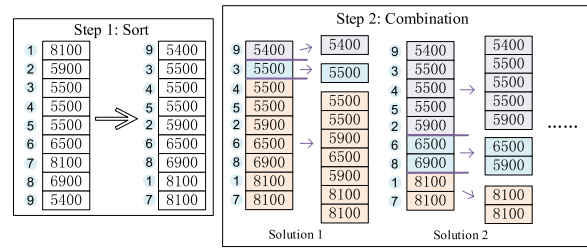


Fig. 6 Search process for the optimal module connection solutions

As the PV array consists of three inverter units, the power output of the overall PV array is the sum of the power generation of each inverter unit, and hence the objective function (f) is defined as:

$$f = P_{array} = \sum_{r=1}^m P_{inv,r} \tag{14}$$

The optimal reconfiguration with the maximum power generation can be obtained through the optimization process over all the candidate reconfigurations for the TCT-based PV array. The pseudo-code is given in “Algorithm1”.

Algorithm1: Dynamical reconfiguration algorithm for a TCT-based PV array.

Input: The irradiance matrix $G_{n \times l}$

The number of inverters r

Output: The optimal connection solution

- 1 **For** $i = 1:n$
- 2 Calculate the sum of string irradiance by (8) and (9);
- 3 Calculate the current generation of each string by (10);
- 4 **end**
- 5 Arranged the sum of irradiance of each PV string from small to large.
- 6 **For** each evaluated connection solution **do**
- 7 **For** $i = 1:r$ **do**
- 8 Calculate power generation with the i -th inverter by (11)
- 9 **end**
- 10 Calculate the sum of the power generation of the PV array by (14).
- 11 **end**
- 12 Select the optimal connection solution with the maximum power generation.

3.3 Application in the SP-based PV array

The proposed dynamic reconfiguration algorithmic solution is also developed for an $N \times L$ SP-based PV array

with m inverters. Based on (1) and (6), the current of each inverter can be expressed as:

$$I_{inv,r} = \sum_{i=1}^t I_{stringi,SP} = \frac{\sum_{i=1}^t \min\{G_{ij}\}}{G_0} I_m \quad (15)$$

where $I_{inv,r}$ represents the current generation of the r th inverter unit on the DC side. $\min\{G_{ij}\}$ is the irradiance received of a PV module in the i th string that is not bypassed. t represents the number of the PV strings that are connected to the r th inverter.

From (7), the power generation of PV strings connected to the r th inverter can be calculated as:

$$P_{inv,r} = I_{inv,r} \times \min\{V_i\} \quad (16)$$

As the PV array consists of m inverter units, the power generation of the overall PV array can also be expressed as (14).

For the SP-based PV array, the combination of simulated annealing (SA) algorithm and genetic algorithm (GA) proposed in [26] is adopted to identify the optimized reconfiguration arrangement and the pseudo-code is given in ‘‘Algorithm2’’. The procedure of optimal reconfiguration solution is as follows:

- (1) Initialization: set an initial high temperature T_0 .
- (2) Obtaining a new solution: a perturbation is given to the current solution to generate a new irradiance matrix solution \mathbf{G}_{new} . ‘Reproduction’, ‘crossover’ and ‘mutation’ in the genetic algorithms are used to generate the perturbation.
- (3) Calculation of the objective function values: according to (14) and (16), the maximum power output of the SP-based PV array corresponding to the current solution is calculated.
- (4) Selection of the solution: based on the Metropolis criterion [27], the probability of the current solution replaced by the new solution is written as:

$$Prob = \begin{cases} 1 & \Delta D > 0 \\ 1/\exp(-\Delta D/T_k) & \Delta D < 0 \end{cases} \quad (17)$$

where $\Delta D = P_{new} - P_{best}$, and T_k is the current simulated annealing temperature of the k th iteration.

- (5) Temperature update: the simulated temperature is updated to a lower value:

$$T_k = T_{k-1} \times \alpha \quad (18)$$

- (6) Termination criterion: repeat steps 2 to 5 until the simulated temperature is lower than the cooling temperature T_n .

- (7) In this algorithm, parameters are related to the complexity and accuracy of the algorithm, and a trade-off is required to set the parameters. In fact, many trials should be conducted to find the parameters correctly [28]. In this work, the parameters are defined as follows: initial temperature $T_0 = 1000$, rate of temperature drop $\alpha = 0.98$ and cooling temperature $T_n = 0.01$.

Algorithm2: Dynamical reconfiguration algorithm for an SP-based PV array.

```

Input: The irradiance matrix  $\mathbf{G}_{m \times l}$ 
          The number of inverters  $r$ 
Output: The optimal irradiance matrix solution  $\mathbf{G}_{solution}$  and
          its optimal connection solution
1 // Initial a high ‘temperature’, a connection solution and an
  objective function value
2  $k = 0$ ;
3  $T_k = 1000$ ;
4  $\mathbf{G}_{solution} = \mathbf{G}_{m \times l}$ ;
5  $P_{best} = 0$ ;
6 If  $T_k > T_n$  do
7 //calculation and comparison of the objective function
  values.
  A perturbation is given to the current solution to generate
  a new irradiance matrix solution  $\mathbf{G}_{new}$ ;
8
9 For each evaluated connection solution of  $\mathbf{G}_{new}$  do
10 For  $i = 1:r$  do
11 Calculate power generation with the  $i^{th}$  inverter
  by (16);
12 end
13 Calculate the power generation of the PV array  $P_{new}$ 
  by (14);
14 end
15 // Select a solution  $\mathbf{G}_{new}$  with the maximum power
  generation  $P_{new}$  based on the Metropolis criterion.
16 If  $Prob > random, 0 \leq random \leq 1$  do
17  $\mathbf{G}_{solution} = \mathbf{G}_{new}$ ;
18  $P_{best} = P_{new}$ ;
19 end
20 // update the ‘temperature’
21  $T_k = T_{k-1} \times \alpha$ ;
22  $k = k + 1$ ;
23 end

```

4 Simulation experiment and numerical results

To evaluate the performance of the proposed dynamic reconfiguration method, the specifications of the PV module used in this paper are shown in Table 2, and the PV arrays with 9×9 TCT and SP interconnections are evaluated under five different mismatch scenarios, as illustrated in Figs. 7 and 8, respectively.

Table 2 PV module specifications

Parameter	Value
Maximum power	83.3 W
Open circuit voltage	12.64 V
Short circuit current	8.62 A
Voltage at the MPP	10.32 V
Current at the MPP	8.07 A

Scenario 1 (long and wide shading): the first four PV strings of the array are under partial shading with four different irradiances (900 W/m², 700 W/m², 400 W/m² and 200 W/m²).

Scenario 2 (double parts shading): two parts of the PV array (the bottom left corner and the center position) are under partial shading with different sizes.

Scenario 3 (long and wide shading with random module failures): additional module failures are considered based on Scenario 1. Here, two PV modules labeled ‘46’ and ‘72’ are assumed to have failed with no output power generation.

Scenario 4 (double parts shading with random module failures): based on Scenario 2, two additional PV modules labeled as ‘55’ and ‘97’ have failed.

Scenario 5 (moving shading with random module failures): based on Scenario 4, nine different shading cases constitute top to bottom shading conditions as illustrated for different mismatch cases in Fig. 8.

For each mismatch scenario, the mismatch losses (ML) of each string in the PV array are calculated and compared for two evaluated topologies, i.e., the proposed dynamical reconfiguration based flexible topology and the three-inverter fixed topology. In addition, the maximum power generation of each string and the MPP of the whole array for both fixed and flexible topologies are simulated and compared using Matlab/Simulink (version 2018a).

ML is defined as the difference between maximum power output under uniform irradiance conditions (MPP_{uni}) and the global maximum power output under mismatch conditions (MPP_{MCS}) [29], determined by (19). In the uniform irradiance condition, the sum of received irradiances is equal to the sum of received irradiances under mismatch conditions.

$$ML = MPP_{uni} - MPP_{MCS} \tag{19}$$

4.1 Simulation experiment for TCT-based PV array

For the TCT-based PV array, the arrangements after carrying out the reconfiguration based on the proposed method for mismatch Scenarios 1 to 4 are presented in Figs. 9a–d, respectively. It can be observed from Fig. 9a that, in Scenario 1, the first inverter is the PV strings that are bypassed. It is shown in Table 3 that the total ML under the mismatch Scenarios 1 to 4, are 7.4 $I_m V_m$, 6.8 $I_m V_m$, 8.8 $I_m V_m$ and 8.2 $I_m V_m$ for the fixed topology. In contrast, the total ML based on the proposed flexible

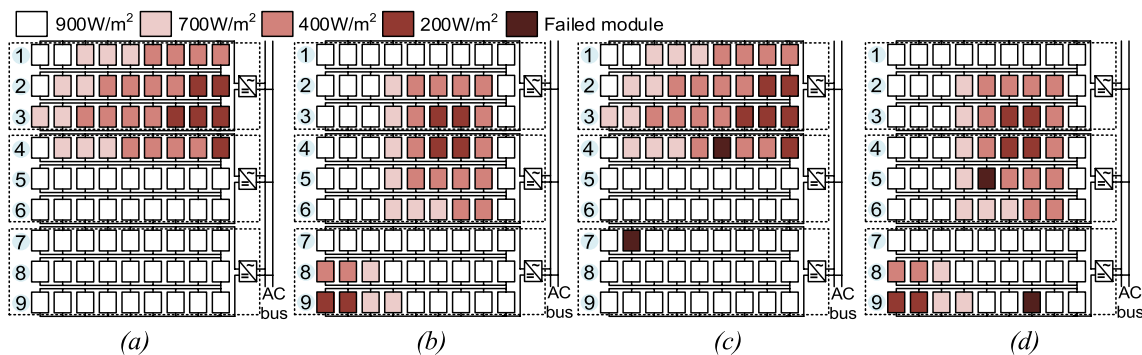


Fig. 7 Four mismatch scenarios (a) Scenario 1 (long and wide shading); (b) Scenario 2 (double parts shading) (c) Scenario 3 (long and wide shading with random modules failure); and (d) Scenario 4 (double parts shading with random failure modules)

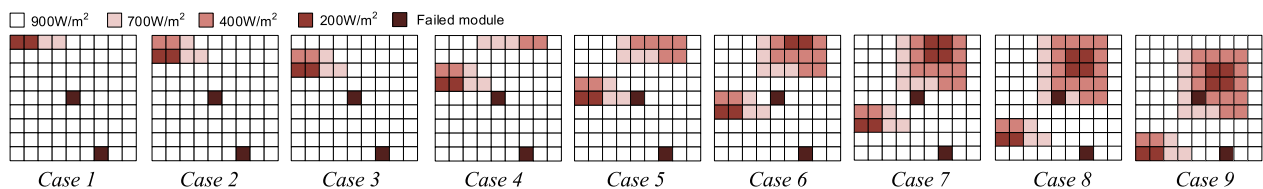


Fig. 8 Shade dispersion of scenario 5 (moving shading with random modules failure)

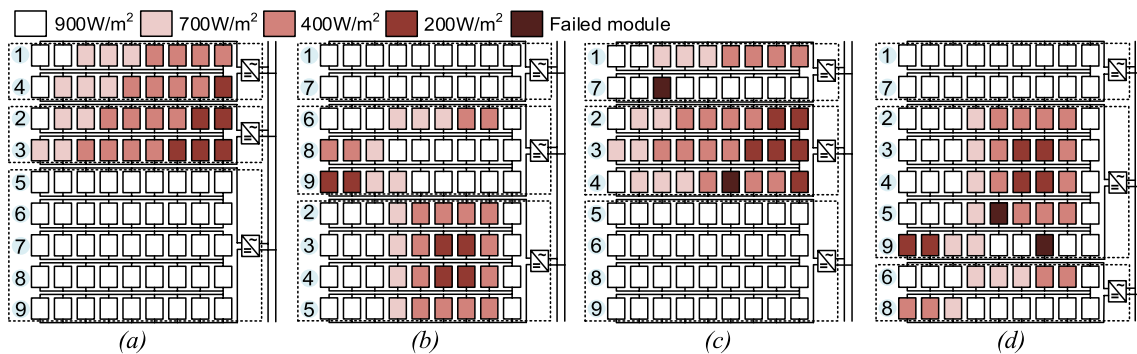


Fig. 9 Arrangement after dynamical reconfiguration for TCT-based PV array (a) Scenario 1; (b) Scenario 2; (c) Scenario 3; and (d) Scenario 4

topology is significantly reduced for all the evaluated scenarios to $1.4 I_m V_m$, $1.6 I_m V_m$, $3.2 I_m V_m$ and $1.2 I_m V_m$, respectively. The time for optimization of the proposed reconfiguration solution for all these tested scenarios is less than 0.02 s.

To further validate the effectiveness of the proposed method, the maximum power generation differences of each string for the two evaluated topologies are shown in Fig. 10. The power difference between different PV strings can be calculated as:

$$\text{Power difference}_{stringi} = P2_{stringi} - P1_{stringi} \quad (20)$$

where $P2_{stringi}$ and $P1_{stringi}$ are the maximum power outputs of the i th string for the proposed flexible topology and the three-inverter fixed topology, respectively. Also, the MPP performances for fixed and flexible topologies are evaluated through simulations, and the results are presented in Fig. 11. It can be seen that the maximum power generations of 55 the proposed flexible topology under four mismatch scenarios are 4841.3 W, 4861.9 W, 4634.3 W, and 4766.3 W, respectively, which are 509.0 W, 276.1 W, 459.9 W and 415.5 W higher than those of the fixed topology. Further, the MPPs of the TCT-connected PV array for 9 cases in Scenario 5 are shown in Fig. 12. For all cases, a maximum enhancement of 11.0% and an average enhancement of 4.74% of power generation can be obtained by the proposed solution.

4.2 Simulation experiment for SP-based PV array

The proposed method for an SP-based PV array is further evaluated, and the four different mismatch scenarios illustrated in Fig. 7 are also used. The detailed arrangements of PV modules in the PV array after array reconfiguration are illustrated in Fig. 13. Also, the ML of individual strings for the fixed and flexible topologies are calculated and compared in Table 4. In this table, some information is simplified in expression, e.g., the horizontal lines divide the string numbers into three parts,

indicating that the PV strings in each part are connected to the same inverter. It can be seen that the total ML of the three-inverter fixed topology for Scenarios 1 to 4 are $8.9 I_m V_m$, $18.3 I_m V_m$, $12.1 I_m V_m$ and $18.1 I_m V_m$, respectively. In comparison, the proposed method provides significant improvement in mismatch conditions with the ML reduced to $6.6 I_m V_m$, $13.4 I_m V_m$, $6.8 I_m V_m$ and $13.0 I_m V_m$, respectively.

To further validate the effectiveness of the proposed dynamic array reconfiguration method, the maximum power difference of individual strings in the PV array is calculated and evaluated for both fixed and flexible topologies, as presented in Fig. 14. Also, the MPP of the whole PV array is simulated and examined, and the results are presented in Fig. 15. It shows that the maximum power generation values of the proposed dynamic reconfiguration based flexible topology under the four mismatch scenarios are 4403.1 W, 3879.4 W, 4274.0 W and 3739.9 W, respectively. The results are 99.5 W, 324.7 W, 221.5 W and 370.4 W higher than those of the fixed topology, with the same mismatch scenarios. The time for optimization of the proposed reconfiguration solution for all the tested scenarios is under 3 s.

In addition, the MPPs of the SP-based PV array for the 9 cases in Scenario 5 are shown in Fig. 16. It can be seen that the maximum power obtained in the proposed flexible topology is improved by 5.55% on average compared to the fixed topology for all the tested cases.

4.3 Cost–benefit analysis for the proposed dynamic PV reconfiguration method

The required hardware of the proposed dynamic PV reconfiguration method mainly includes the PV monitoring instruments, switching matrix and driving circuits [10]. The prices of the chosen components are shown in Table 5. Note that the selected measuring instruments, i.e., voltage and current sensors, are useful for PV panels

Table 3 The ML of PV array of fixed and flexible topologies for the four scenarios

Fixed topology				Flexible topology				Fixed topology				Flexible topology			
Inverter No	String No	Power (lmVm)	ML (lmVm)	Inverter No	String No	Power (lmVm)	ML (lmVm)	Inverter No	String No	Power (lmVm)	ML (lmVm)	Inverter No	String No	Power (lmVm)	ML (lmVm)
Scenario 1															
1	1	5.5	1.9	1	1	5.5	0.7	1	1	8.1	2.6	1	1	8.1	0.0
2	4.3	0.7	0.0	4	4.8	0.0	0.0	2	2	5.9	0.4	7	7	8.1	0.0
3	3.6	0.0	0.0	2	4.3	0.7	0.7	3	3	5.5	0.0	2	6	6.5	0.2
4	4.8	0.0	4.8	3	3.6	0.0	0.0	2	4	5.5	0.0	8	8	6.9	0.6
5	8.1	0.0	0.0	5	8.1	0.0	0.0	5	5	5.9	0.4	9	9	6.3	0.0
6	8.1	0.0	0.0	6	8.1	0.0	0.0	6	6	6.5	1.0	3	2	5.9	0.4
7	8.1	0.0	0.0	7	8.1	0.0	0.0	3	7	8.1	1.8	3	3	5.5	0.0
8	8.1	0.0	0.0	8	8.1	0.0	0.0	8	8	6.9	0.6	4	4	5.5	0.0
9	8.1	0.0	0.0	9	8.1	0.0	0.0	9	9	6.3	0.0	5	5	5.9	0.4
Scenario 2															
Scenario 3															
1	1	5.5	1.9	1	1	5.5	0.0	1	1	8.1	2.6	1	1	8.1	0.0
2	4.3	0.7	0.0	7	7.2	1.7	1.7	2	2	5.9	0.4	7	7	8.1	0.0
3	3.6	0.0	0.0	2	4.3	0.7	0.7	3	3	5.5	0.0	2	2	5.9	0.5
4	4.4	0.0	4.4	3	3.6	0.0	0.0	2	4	5.5	0.0	3	3	5.5	0.1
5	8.1	0.0	0.0	4	4.4	0.8	0.8	5	5	5.5	0.0	4	4	5.5	0.1
6	8.1	0.0	0.0	5	8.1	0.0	0.0	6	6	6.5	1.0	5	5	5.5	0.1
7	7.2	0.0	0.0	6	8.1	0.0	0.0	3	7	8.1	2.7	9	9	5.4	0.0
8	8.1	0.9	0.9	8	8.1	0.0	0.0	8	8	6.9	1.5	3	6	6.5	0.0
9	8.1	0.9	0.9	9	8.1	0.0	0.0	9	9	5.4	0.0	8	8	6.9	0.4

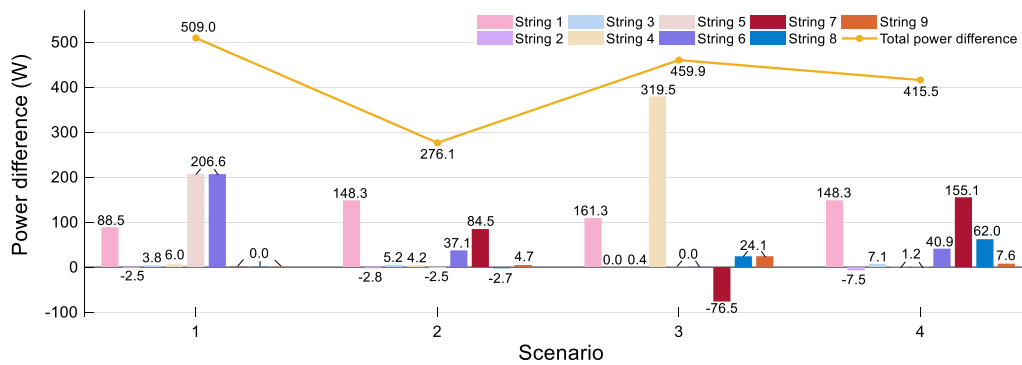


Fig. 10 Maximum power difference of each string between the two evaluated topologies and the total maximum power difference

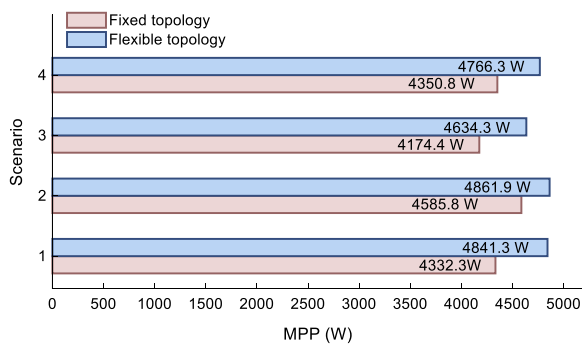


Fig. 11 MPP performance comparison under the four mismatch scenarios

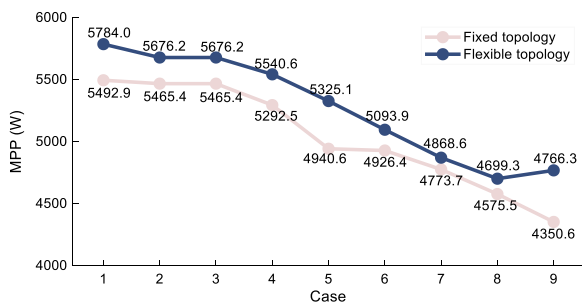


Fig. 12 MPPs of the TCT connected PV array for the 9 cases in Scenario 5

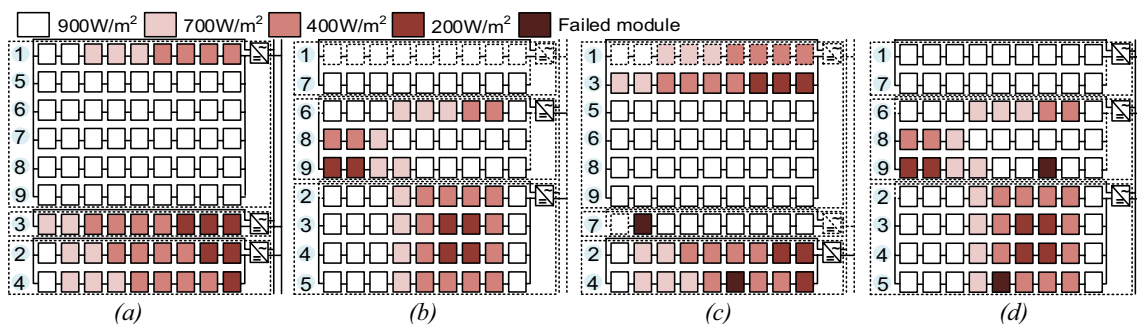


Fig. 13 Arrangement after dynamical reconfiguration for SP-based PV array (a) Scenario 1; (b) Scenario 2; (c) Scenario 3; and (d) Scenario 4

with a voltage range of between 0 and 25 V and current range between 0 and 20 A [30]. In the switching matrix, each switch consists of an electromechanical relay and one or several semiconductor devices, e.g., MOSFETs. One MOSFET has to be connected to each relay with a driver required for controlling the MOSFET [10].

The number of required components which should be used in the 9×9 and 9×20 TCT and SP interconnected PV arrays with three inverters are shown in Table 6, as well as the total installation cost. As mentioned above, the size of the switching matrix is only determined by the numbers of the PV strings and inverters. Therefore, for the 9×20 PV array, the number of relays, MOSFETs and drivers required will not increase.

As mentioned in the introduction, the mismatch losses problem will occur because of module non-uniform aging, module failure and shading. Except for the shading caused by surrounding buildings, the other factors are random and therefore the increment obtained by the dynamic reconfiguration method is hard to estimate. Indeed, the increment of power generation depends on the degree of non-uniform aging, the position of the failed modules, the size and location of shadings as well as the topology of the PV array. For this reason, in this work, for a PV array of 25 years' life, working time of five

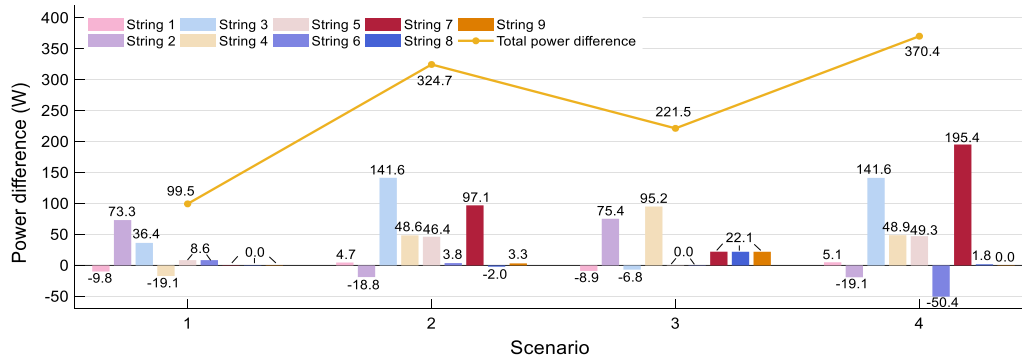


Fig. 14 Maximum power difference of each string between the two evaluated topologies and the total maximum power difference

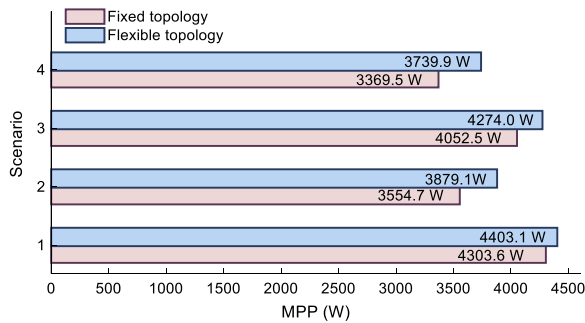


Fig. 15 MPP of the fixed and flexible topologies for SP-based PV array under the four mismatch scenarios

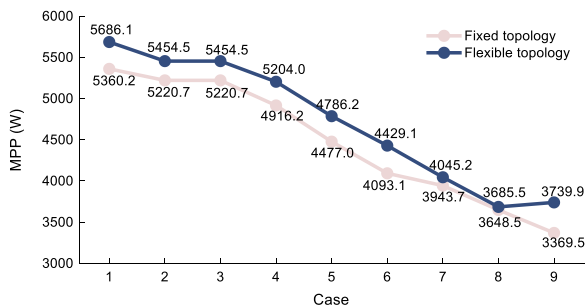


Fig. 16 MPPs of the SP-based PV array for the 9 cases in Scenario 5

Table 5 Price of the required hardware of the dynamic PV reconfiguration method

Component	Brand	Price (\$)
Voltage sensor	MF301	0.38
Current sensor	ACS712	1.30
Relay	Hongfa Europe GmbH	2.95
MOSFET	IPB08CN10N	1.44
Driver	MAX845	3.63

Table 6 Components considered for each topology

Topologies	TCT		SP	
	9 × 9	9 × 20	9 × 9	9 × 20
Voltage sensor	81	180	81	180
Current sensor	81	180	81	180
Relay	77	77	48	48
MOSFET	77	77	48	48
Driver	77	77	48	48
Total cost (\$)	753.62	919.94	521.04	687.36

hours per day, and an average power reduction of 35% is considered, and the same value of power increment has been considered for each topology and fixed to 5% for simplicity [10]. The economic analysis of the reconfiguration method is calculated as \$83 per megawatt hour (MWh), which is the weighted average wholesale price for solar PV-generated electricity in the USA in 2019 [31].

To further assess the cost-benefit for module types with different capacities, an analysis of module capacity of 83 kW, 150 kW and 250 kW is carried out. Considering a PV array lifetime of 25 years, for the 9 × 9 and 9 × 20 TCT and SP interconnected PV arrays, the economic estimates of the proposed reconfiguration method are shown in Tables 7 and 8, respectively. It can be seen that the benefit of the PV array increases with the increase of the module capacity and the number of PV modules in a string. In addition, the deployment of the proposed reconfiguration method can enhance the condition monitoring and analysis of the operating PV modules, and improve the maintenance of the PV systems [32].

Table 7 The economic estimates of the proposed reconfiguration method for TCT-based PV array

After n years		$n = 5$	$n = 10$	$n = 15$	$n = 20$	$n = 25$
Size	Power	Benefit (\$)				
9×9	83	-588.1	-422.7	-257.2	-91.7	73.8
	150	-454.6	-155.5	143.6	442.7	741.7
	250	-255.2	243.3	741.7	1240.2	1738.6
9×20	83	-552.2	-184.5	183.3	551	918.8
	150	-255.3	409.3	1073.8	1738.4	2403
	250	187.7	1295.4	2403	3510.7	4618.4

Table 8 The economic estimates of the proposed reconfiguration method for SP-based PV array

After n years		$n = 5$	$n = 10$	$n = 15$	$n = 20$	$n = 25$
Size	Power	Benefit (\$)				
9×9	83	-355.6	-190.1	-24.6	140.9	306.4
	150	-222	77.1	376.2	675.2	974.3
	250	-22.6	475.9	974.3	1472.7	1971.2
9×20	83	-319.6	48.1	415.9	783.6	1151.4
	150	-22.8	641.8	1306.4	1971	2635.6
	250	420.3	1528	2635.6	3743.3	4850.9

5 Conclusion and future work

In this paper, a dynamic array reconfiguration method is developed to improve the maximum output power generation for any size of distributed PV array with TCT or SP interconnections, in different mismatch conditions. The schematic of the switching matrix for TCT and SP interconnected PV arrays is developed to achieve flexible connections between PV strings and inverters. The proposed reconfiguration solution is implemented by controlling the switching matrix to dynamically alter the electrical connections according to the mismatch conditions. The proposed method is assessed through simulations for a range of mismatch conditions due to partial shading and random module failures. The numerical results demonstrate that the proposed method outperforms the benchmark for all evaluated mismatch scenarios, with average MPP improved by 8.56% for the TCT-based PV array and 6.43% for the SP-based PV array compared to the fixed topology scheme.

Acknowledgements

Not applicable

Author contributions

XF: Conceptualization, Methodology, Data curation, Writing, Original draft preparation. QY: Supervision, Reviewing and Editing, WY: Investigation, Visualization. All authors read and approved the final manuscript.

Author informations

Xiaolun Fang (1996-), female, Major in Control Science and Control engineering. Her research area includes the operational management of renewable energy systems.

Qiang Yang (1979-), male, PHD and Professor, Major in Electrical Engineering. His research area includes the data analytics and control of complex energy systems.

Wenjun Yan (1964-), male, PHD and Professor, Major in Control Science and Control engineering. His research area includes the operational control and management of complex energy systems.

Funding

This work is support in part by the Technology Research and Development Program of Zhejiang Province (2022C01239), the National Natural Science Foundation of China (52177119) and the Fundamental Research Funds for the Central Universities (Zhejiang University NGICS Platform).

Availability of data and materials

Not applicable.

Declarations

Competing interests

The authors declare that they have no known competing financial interests or personal relationships that could have appeared to influence the work reported in this paper.

Author details

¹College of Electrical Engineering, Zhejiang University, Hangzhou 310027, China. ²Zhejiang Lab, Hangzhou 310000, China.

Received: 17 February 2022 Accepted: 1 August 2022

Published online: 05 September 2022

References

- Iqbal, B., Nasir, A., & Murtaza, A. F. (2021). Stochastic maximum power point tracking of photovoltaic energy system under partial shading conditions. *Protection and Control of Modern Power Systems*. <https://doi.org/10.1186/s41601-021-00208-9>
- Zhao, Y., An, A., Xu, Y., et al. (2021). Model predictive control of grid-connected PV power generation system considering optimal MPPT control of PV modules. *Protection and Control of Modern Power Systems*. <https://doi.org/10.1186/s41601-021-00210-1>
- China Energy Portal. (2020). *PV installation and operational in the first half of 2020*. Available: <https://chinaenergyportal.org/2020-q2-pv-installations-utility-and-distributed-by-province/>
- Lappalainen, K., & Velkealahti, S. (2017). Photovoltaic mismatch losses caused by moving clouds. *Solar Energy*, *158*, 455–461.
- Krishna, G. S., & Moger, T. (2019). Reconfiguration strategies for reducing partial shading effects in photovoltaic arrays: State of the art. *Solar Energy*, *182*, 429–452.
- Rani, B. I., Ilango, G. S., & Nagamani, C. (2013). Enhanced power generation from PV array under partial shading conditions by shade dispersion using Su Do Ku configuration. *IEEE Transactions on Sustainable Energy*, *4*, 594–601.
- Krishna, S. G., & Moger, T. (2019). Optimal SuDoKu reconfiguration technique for total-cross-tied PV array to increase power output under non-uniform irradiance. *IEEE Transactions on Energy Conversion*, *34*, 1–12.
- Bosco, M. J., & Mabel, M. C. (2017). A novel cross diagonal view configuration of a PV system under partial shading condition. *Solar Energy*, *158*, 760–773.
- Hu, Y., Zhang, J., Li, P., Yu, D., & Jiang, L. (2017). Non-uniform aged modules reconfiguration for large-scale PV array. *IEEE Transactions on Device and Materials Reliability*, *17*, 560–569.
- Schettino, G., Pellitteri, F., Ala, G., Miceli, R., Romano, P., & Viola, F. (2020). PV reconfiguration systems: a technical and economic study. *Energies*, *13*, 1–21.
- Babu, T. S., Ram, J. P., Dragičević, T., Miyatake, M., Blaabjerg, F., & Rajasekar, N. (2018). Particle swarm optimization based solar PV array reconfiguration of the maximum power extraction under partial shading conditions. *IEEE Transactions on Sustainable Energy*, *9*, 74–85.
- Deshkar, S. N., Dhale, S. B., Mukherjee, J. S., Babu, T. S., & Rajasekar, N. (2015). Solar PV array reconfiguration under partial shading conditions for maximum power extraction using genetic algorithm. *Renewable and Sustainable Energy Reviews*, *43*, 102–110.
- Yousri, D., Babu, T. S., Mirjalili, S., Rajasekar, N., & Elaziz, M. A. (2020). A novel objective function with artificial ecosystem-based optimization for relieving the mismatching power loss of large-scale photovoltaic array. *Energy Conversion and Management*. <https://doi.org/10.1016/j.enconman.2020.113385>
- Fathy, A. (2020). Butterfly optimization algorithm based methodology for enhancing the shaded photovoltaic array extracted power via reconfiguration process. *Energy Conversion and Management*. <https://doi.org/10.1016/j.enconman.2020.113115>
- Ajmal, A. M., Ramachandramurthy, V. K., Naderipour, A., & Ekanayake, J. B. (2021). Comparative analysis of two-step GA-based PV array reconfiguration technique and other reconfiguration techniques. *Energy Conversion and Management*, *230*, 113806.
- Karakose, M., Baygin, M., Baygin, N., Murat, K., & Akin, E. (2014). An intelligent reconfiguration approach based on fuzzy partitioning in PV arrays. In *2014 IEEE International Symposium on Innovations in Intelligent Systems and Applications*, (pp. 356–360). Alberobello.
- Parlak, K. S., & Karaköse, M. (2014). An efficient reconfiguration method based on standard deviation for series and parallel connected PV arrays. In *2014 International Conference on Renewable Energy Research and Application*, (pp. 457–461). Milwaukee, WI.
- Alahmad, M., Chaaban, M. A., Lau, S., Shi, J., & Neal, J. (2012). An adaptive utility interactive photovoltaic system based on a flexible switch matrix to optimize performance in real-time. *Solar energy*, *86*, 951–963.
- Storey, J., Wilson, P. R., & Bagnall, D. (2014). The optimized-string dynamic photovoltaic array. *IEEE Transactions on Power Electronics*, *29*, 1768–1776.
- Meerimatha, G., & Loveswara Rao, B. (2020). Novel reconfiguration approach to reduce line losses of the photovoltaic array under various shading conditions. *Energy*, *196*, 117–120.
- Satpathy, P. R., Sharma, R., & Jena, S. (2017). A shade dispersion interconnection scheme for partially shaded modules in a solar PV array network. *Energy*, *139*, 350–365.
- Satpathy, P. R., & Sharma, R. (2019). Power and mismatch losses mitigation by a fixed electrical reconfiguration technique for partially shaded photovoltaic arrays. *Energy Conversion and Management*, *192*, 52–70.
- Tang, R., Lin, Q., Zhou, J., Zhang, S., Lai, J., Li, X., & Dong, Z. (2020). Suppression strategy of short-term and long-term environmental disturbances for maritime photovoltaic system. *Applied Energy*, *259*, 114–183.
- Mansur, A. A., Amin, M. R., Islam, K. K. (2019). Determination of module rearrangement techniques for non-uniformly aged PV arrays with SP, TCT, BL and HC configurations for maximum power output. In *International Conference on Electrical, Computer and Communication Engineering*, (pp. 1–5), Cox's Bazar: Bangladesh.
- Velasco-Quesada, G., Guinjoan-Gispert, F., Pique-Lopez, R., Roman-Lumbreras, M., & Conesa-Roca, A. (2009). Electrical PV array reconfiguration strategy for energy extraction improvement in grid-connected PV systems. *IEEE Transactions on Industrial Electronics*, *56*, 4319–4331.
- Fang, X., Yang, Q., & Yan, W. (2021). Switching matrix enabled optimal topology reconfiguration for maximizing power generation in series-parallel organized photovoltaic systems. In *IEEE Systems Journal* (pp. 1–11).
- Jiang, C., & Wang, C. (2015). Improved evolutionary programming with dynamic mutation and metropolis criteria for multi-objective reactive power optimization. *IEEE Proceedings-Generation, Transmission and Distribution*, *152*, 291–294.
- Wang, J., Jin, G., Wang, Y., & Chen, X. (2009). Genetic simulated annealing algorithm used for PID parameters optimization. In *2009 International Conference on Artificial Intelligence and Computational Intelligence*, (pp. 397–401), Shanghai.
- Krishna, G. S., & Moger, T. (2019). Improved Sudoku reconfiguration technique for total-cross-tied PV array to enhance maximum power under partial shading conditions. *Renewable and Sustainable Energy Reviews*, *109*, 333–348.
- Hall Current Sensor Module ACS712 module, Available online: <https://www.aliexpress.com>
- Solar PV generators receive higher electricity prices than other technologies – EIA, Available online: <https://renewablesnow.com/news/solar-pv-generators-receive-higher-electricity-prices-than-other-technologies-eia-716914/>
- Hammoumi, A. E., Motahhir, S., Chalh, A., Ghzizal, A. E., & Derouich, A. (2018). Low-cost virtual instrumentation of PV panel characteristics using Excel and Arduino in comparison with traditional instrumentation. *Renewables Wind Water & Solar*, *5*, 1–16.